

Combining model calibration and design

Carl Ehrett*

School of Mathematical and Statistical Sciences, Clemson University,

D. Andrew Brown

School of Mathematical and Statistical Sciences, Clemson University,

Evan Chodora

Department of Mechanical Engineering, Clemson University,

Christopher Kitchens

Department of Chemical and Biomolecular Engineering, Clemson University,

and

Sez Atamturktur

Department of Architectural Engineering, Pennsylvania State University

Keywords:

*The authors gratefully acknowledge *please remember to list all relevant funding sources in the unblinded version*

1 Introduction

The goal of traditional Kennedy-O’Hagan style calibration (KOH, Kennedy and O’Hagan, 2001) is to find a posterior distribution on unknown parameters by calibrating a computer model using real-world observations of the modeled phenomenon. By contrast, the design methodology of calibration to target outcomes (CTO) uses the KOH framework to find a posterior distribution on optimal input settings in the model by “calibrating” a computer model using artificial observations that reflect performance and cost targets for the modeled system. The goal of the work described here is to combine KOH and CTO. Call the resulting methodology DCTO, for dual calibration to target outcomes.

CTO as previously developed assumes, somewhat idealistically, that the computer model is already perfectly calibrated. DCTO avoids this idealization. Furthermore, when undertaking KOH, some areas of the model range may be of greater interest than others. For example, one may be more interested in calibrating the model to be accurate in the optimal region of some design variable θ than elsewhere. Undertaking dual calibration may allow us to focus our calibration efforts on such regions of interest, prioritizing them over other areas of the model range.

2 The model

Let f be the model of interest, and partition its inputs as (x, θ_1, θ_2) where x denotes the known and/or controllable inputs, θ_1 denotes the parameters targeted for KOH calibration, and θ_2 denotes the input settings targeted for design via CTO. If f can be run quickly,

then we use it directly in MCMC. However, if it is computationally expensive, we employ a surrogate by setting a Gaussian process (GP) prior on f with mean $m_0(x, t_1, t_2)$ and covariance function $C_0((x, t_1, t_2), (x', t'_1, t'_2))$. From here on in this discussion, assume that a GP surrogate is used for f . Typically, there will be some systematic discrepancy between the output of f and the true system, even if the true value of θ_1 is used. We model this discrepancy, between the true system and f at the true value of θ_1 , with another GP prior δ_1 having mean $m_1(x, t_2)$ and covariance function $C_1((x, t_2), (x', t'_2))$. In addition to the discrepancy between f and the true system, there may also be a systematic discrepancy between the true system and our performance/cost targets, particularly if the latter are especially optimistic. We model this discrepancy using a GP prior with mean $m_2(x)$ and covariance function $C_2(x, x')$. Notice that this discrepancy is between the true system at optimal settings for θ_2 and f using the true value of θ_1 and the optimal settings for θ_2 . In addition to systematic discrepancy between f and reality, measurement error must be included in the model. Thus let $\epsilon \sim N(0, \sigma^2)$ denote the (known) i.i.d. variance of (real) observations at any given values of x, t_2 . Finally, we assume that η, δ_1, δ_2 , and ϵ are all mutually independent.

A collection of simulation runs is needed to train the GP code surrogate. Let $(\mathbf{x}_s, \mathbf{t}_{1s}, \mathbf{t}_{2s})$ be the design matrix for these simulation runs, and let \mathbf{y}_s denote the output of these runs. Similarly, let \mathbf{y}_r be the real observations at $\mathbf{x}_r, \mathbf{t}_{2r}$, and let \mathbf{y}_d be a set of artificial “observations” reflecting our cost and performance targets at control settings \mathbf{x}_d . Call \mathbf{y}_d the *target outcomes*. Finally, let $\mathbf{y} = (\mathbf{y}_s, \mathbf{y}_r, \mathbf{y}_d)^T$. Then it follows that $\mathbf{y} \sim N(\mathbf{m}, \mathbf{C})$,

where

$$\mathbf{m} = \begin{pmatrix} m_0(\mathbf{x}_s, \mathbf{t}_{1s}, \mathbf{t}_{2s}) \\ m_0(\mathbf{x}_r, \mathbf{1}\theta_1, \mathbf{t}_{2r}) + m_1(\mathbf{x}_1, \mathbf{t}_{2r}) \\ m_0(\mathbf{x}_d, \mathbf{1}\theta_1, \mathbf{1}\theta_2) + m_1(\mathbf{x}_d, \mathbf{1}\theta_2) + m_2(\mathbf{x}_d) \end{pmatrix},$$

$$\mathbf{C} = \begin{pmatrix} \mathbf{C}_{11} & \mathbf{C}_{12} & \mathbf{C}_{13} \\ \mathbf{C}_{21} & \mathbf{C}_{22} & \mathbf{C}_{23} \\ \mathbf{C}_{31} & \mathbf{C}_{32} & \mathbf{C}_{33} \end{pmatrix},$$

$$\mathbf{C}_{11} = C_0((\mathbf{x}_s, \mathbf{t}_{1s}, \mathbf{t}_{2s}), (\mathbf{x}_s, \mathbf{t}_{1s}, \mathbf{t}_{2s}))$$

$$\mathbf{C}_{21} = C_0((\mathbf{x}_s, \mathbf{t}_{1s}, \mathbf{t}_{2s}), (\mathbf{x}_r, \mathbf{1}\theta_1, \mathbf{t}_{2r}))$$

$$\mathbf{C}_{31} = C_0((\mathbf{x}_s, \mathbf{t}_{1s}, \mathbf{t}_{2s}), (\mathbf{x}_d, \mathbf{1}\theta_1, \mathbf{1}\theta_2))$$

$$\mathbf{C}_{12} = \mathbf{C}_{21}^T$$

$$\mathbf{C}_{22} = C_0((\mathbf{x}_r, \mathbf{1}\theta_1, \mathbf{t}_{2r}), (\mathbf{x}_r, \mathbf{1}\theta_1, \mathbf{t}_{2r})) + C_1((\mathbf{x}_r, \mathbf{t}_{2r}), (\mathbf{x}_r, \mathbf{t}_{2r})) + \sigma_2 \mathbf{I}$$

$$\mathbf{C}_{32} = C_0((\mathbf{x}_r, \mathbf{1}\theta_1, \mathbf{t}_{2r}), (\mathbf{x}_d, \mathbf{1}\theta_1, \mathbf{1}\theta_2)) + C_1((\mathbf{x}_r, \mathbf{t}_{2r}), (\mathbf{x}_d, \mathbf{1}\theta_2))$$

$$\mathbf{C}_{13} = \mathbf{C}_{31}^T$$

$$\mathbf{C}_{23} = \mathbf{C}_{32}^T$$

$$\mathbf{C}_{33} = C_0((\mathbf{x}_s, \mathbf{1}\theta_1, \mathbf{1}\theta_2), (\mathbf{x}_s, \mathbf{1}\theta_1, \mathbf{1}\theta_2)) + C_1((\mathbf{x}_s, \mathbf{1}\theta_2), (\mathbf{x}_s, \mathbf{1}\theta_2)) + C_2(\mathbf{x}_d, \mathbf{x}_d)$$

Note that when \mathbf{y}_d and \mathbf{x}_d are empty and \mathbf{m}, \mathbf{C} reduce respectively to their first two and upper two-by-two block elements, this is simply the KOH framework. Thus, DCTO generalizes the KOH framework.

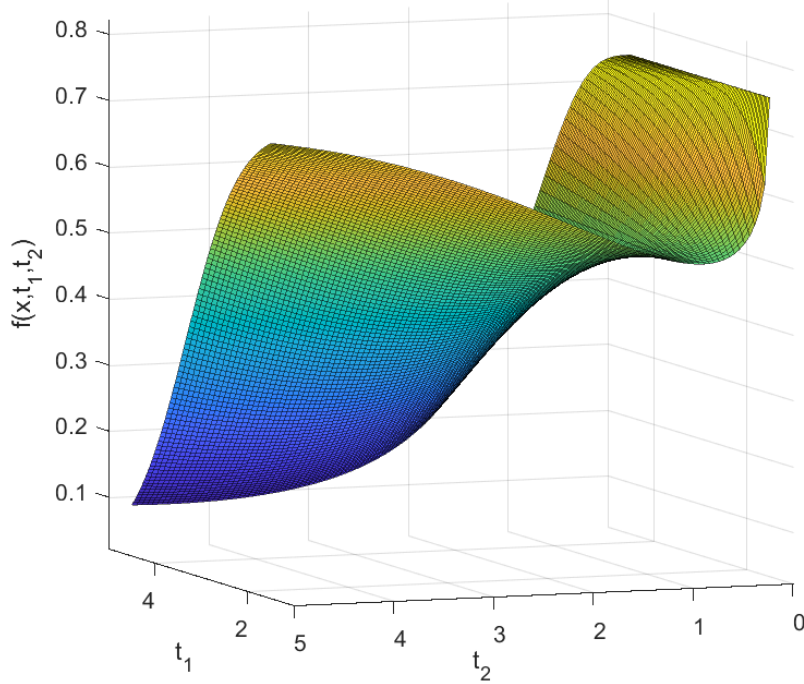


Figure 1: Example computer model output over the support of the calibration parameter t_1 and the design parameter t_2 .

3 Example with simulated data

Consider the function of three inputs $f(x, t_1, t_2) = x/(t_2^{t_1-1} \exp(-0.75t_2) + 1)$. Figure 1 shows the output of this function for $x = 1$ over the range $(t_1, t_2) \in [1.5, 4.5] \times [0, 5]$. We arbitrarily set $\theta_1 = 2$ to be the “true” value of t_1 . For any value of x and t_1 , the optimal (minimizing) value of t_2 is $(4/3)(t_1 - 1)$, so we have $\theta_2 = 4/3$. Figure 2 shows the locations of the true and optimal values (respectively) of θ_1 and θ_2 . There it is clear that the true value of θ_1 is far from optimal – if this value were within our control, its optimal value would be at the upper end of its support, at 4.5. Thus f showcases the ability of DCTO to perform simultaneously both calibration and design in the case when our “truth-seeking” goals and our design goals are in tension.

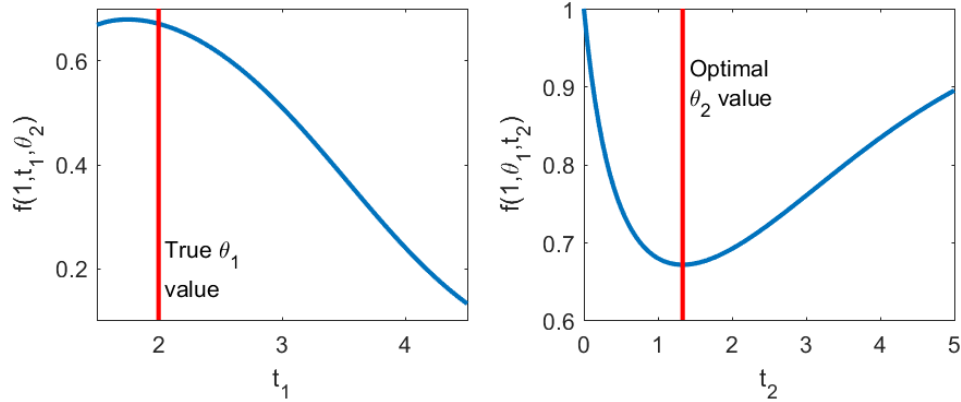


Figure 2: The lefthand plot shows the computer model output at $x = 1$ and optimal θ_2 for each value of the calibration parameter t_1 . The righthand plot shows the model output at $x = 1, t_1 = \theta_1$ for each value of the design parameter t_2 .

3.1 Results

We used DCTO on four versions of the problem. First, we assumed that f is free from discrepancy – i.e. that $f(x, \theta_1, t_2)$ is an unbiased estimator of the “true” system $g(x, t_2)$. The other three versions each assume that f suffers from some form of discrepancy. Let g_1, g_2, g_3 denote the “true” systems in these three cases. We set

$$\begin{aligned}
 g_1(x, t_2) &= f(x, \theta_1, t_2) (1 - c(x - .5)(x - 1)/x)) \\
 g_2(x, t_2) &= f(x, \theta_1, t_2) - c(x - .5)(x - 1) \left(t_2 - \frac{4}{3} \right)^2 + d \\
 g_3(x, t_2) &= f(x, \theta_1, t_2) + cxt_2 + d
 \end{aligned}$$

Where c, d are constants which determine how severe the discrepancy is in each case. The function g_1 has a multiplicative discrepancy dependent only on x . This discrepancy does not affect the optimal value of t_2 . The discrepancy of g_2 is additive, and is dependent

upon both x and θ_1 . Though this discrepancy can affect the optimal value of t_2 , in the case that $\theta_1 = 2$ (which is what we assume to be the truth) it does not. Thus under g_1 and g_2 , it remains the case that the optimal value of t_2 is $\theta_2 = 4/3$. By contrast, g_3 has an additive discrepancy which does affect the optimal setting for t_2 . For g_3 , optimal t_2 is dependent upon both the true value of θ_1 and upon the value of c . For example, for $\theta_1 = 2$ and $c = 0.055$, the optimal t_2 is $\theta_2 \approx 1$. Figure 3 shows the discrepancies for two different versions (corresponding to different settings of (c, d)) of each g_i .

We applied DCTO to each of seven cases: the non-discrepancy case, and the two different versions of each g_i shown in Figure 3. We found that in these cases, no appreciable difference resulted from the decision of whether or not to use an emulator (where the emulator was trained on a latin hypercube design of 250 points on the space of model inputs). Therefore, the results reported here do not employ an emulator. In each case, we gathered 50 “observations” of g_i on a latin hypercube design over the supports of x and θ_2 , setting θ_1 equal to its “true” value of 2. After standardizing the response to have mean 0 and standard deviation 1, we added i.i.d. $N(0, 0.05)$ noise to the response. We then carried out DCTO using Metropolis-Hastings-within-Gibbs MCMC, drawing 8000 samples each of $t_1, t_2, \boldsymbol{\rho}_{\delta_1}, \lambda_{\delta_1}, \rho_{\delta_2}, \lambda_{\delta_2}$, where the latter four are the hyperparameters of the product power exponential covariance functions C_1 and C_2 . In order to evaluate the success of the calibration component of DCTO, we also carried out a two-step procedure of using traditional KOH calibration of θ_1 , followed by a second step using CTO to obtain a distribution of θ_2 . The first step is essentially DCTO with $\mathbf{x}_d, \mathbf{y}_d$ as empty (null) vectors, and the second step uses the distribution obtained in the first step to estimate θ_2 . Thus, the compari-

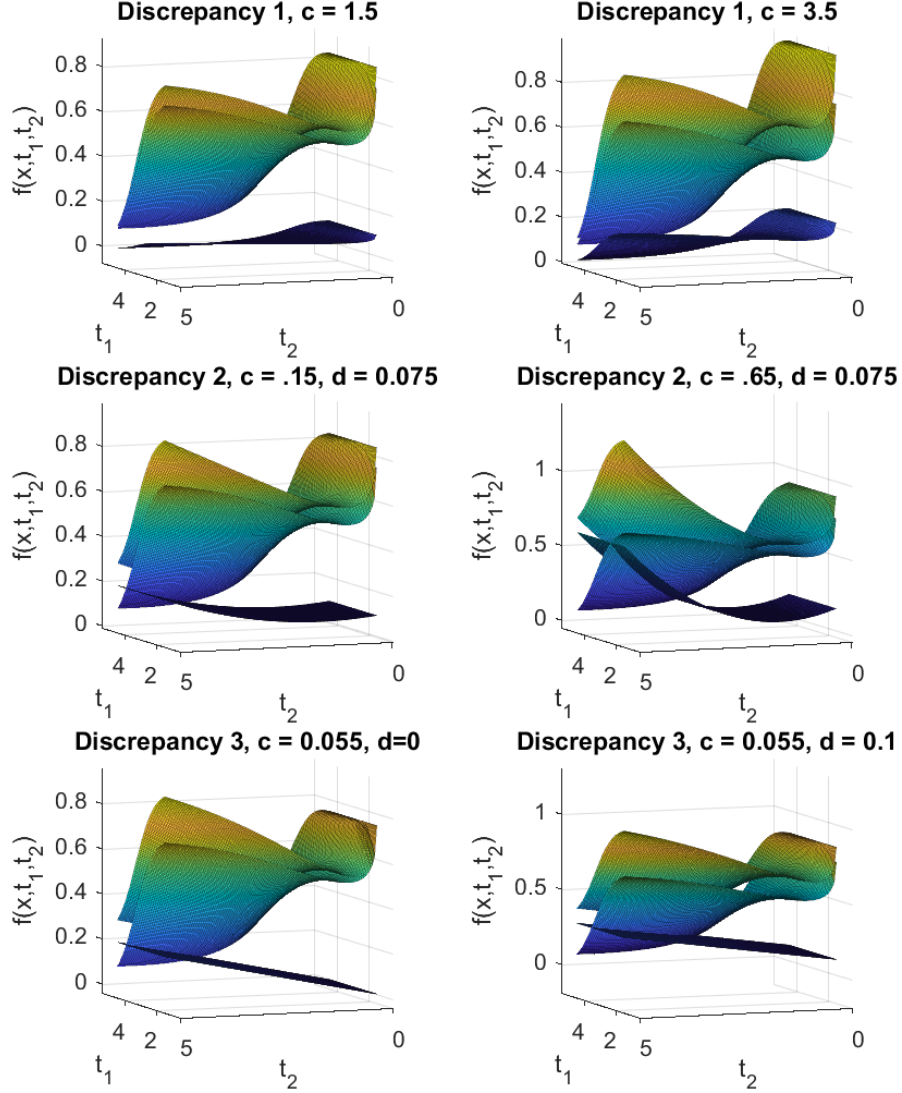


Figure 3: The i^{th} row shows g_i (the objective function with discrepancy), f (the computer model), and the discrepancy $g_i - f$, all at $x = 0.75$. In each row, a less aggressive version of the discrepancy appears on the left, and a more aggressive on the right. In each plot, the topmost surface is g_i , the middle surface is f , and the bottom surface is the discrepancy $g_i - f$.

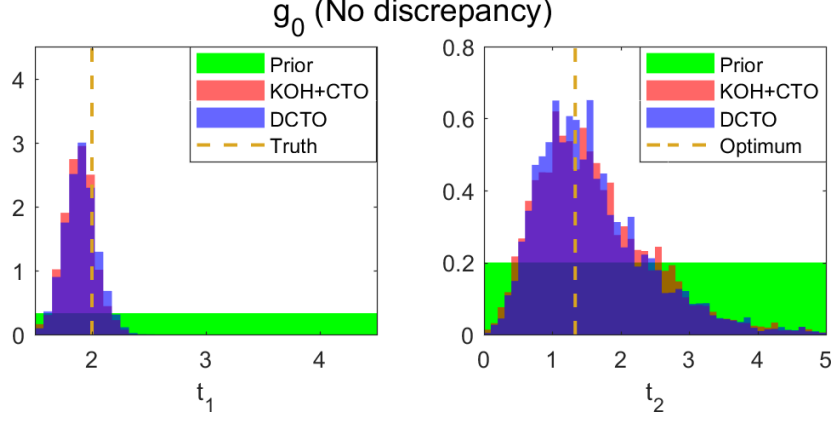


Figure 4: Prior and posterior distributions of the calibration parameter θ_1 and design parameter θ_2 , along with their true/optimal values, for DCTO and KOH+CTO carried out when there is no discrepancy between the true system and the computer model.

son between DCTO and KOH+CTO shows the difference between DCTO and performing CTO on a system which has been calibrated using traditional methods. Figure 4 shows the results for g_0 , the case of no discrepancy. The two methods deliver comparable results, showing that combining KOH calibration and CTO design into DCTO does not undermine the performance of either task. Strong Bayesian learning has occurred for both parameters, in that the posterior distributions of θ_1, θ_2 are peaked around their true and optimal values, respectively. KOH gives a similar posterior for θ_1 , showing that the expansion of DCTO to undertake design has not interfered with its calibration performance. The skewness apparent in the posterior distributions of θ_2 occur in all of the results gathered here, and is likely due to the shape of the objective function f , which increases sharply for $t_2 < \theta_2$ and increases much more gently for $t_2 > \theta_2$.

Figure 5 shows the results for g_1 at two settings of c , and Figure 6 shows the results for g_2 at two settings of (c, d) . Somewhat counterintuitively, even stronger Bayesian learning occurs with respect to θ_1 in the case of g_1 than in the case of g_0 , in each of the

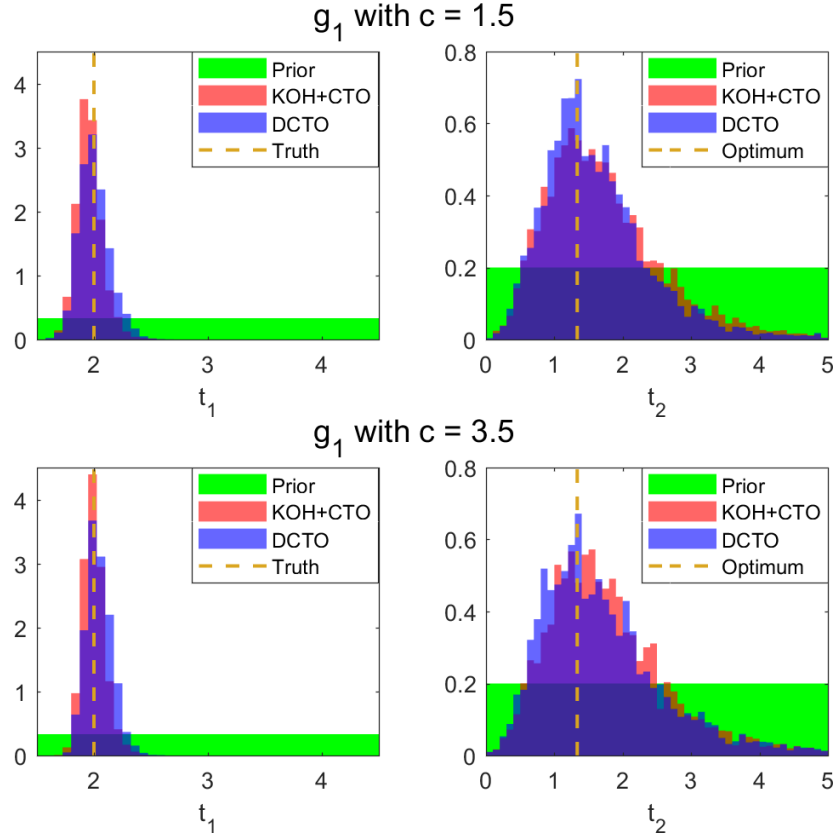


Figure 5: Prior and posterior distributions of the calibration parameter θ_1 and design parameter θ_2 , along with their true/optimal values, for DCTO and KOH+CTO in the case of true systems g_1 . The top row corresponds to a smaller discrepancy, with $c = 1.5$; the bottom row corresponds to a larger discrepancy, with $c = 3.5$.

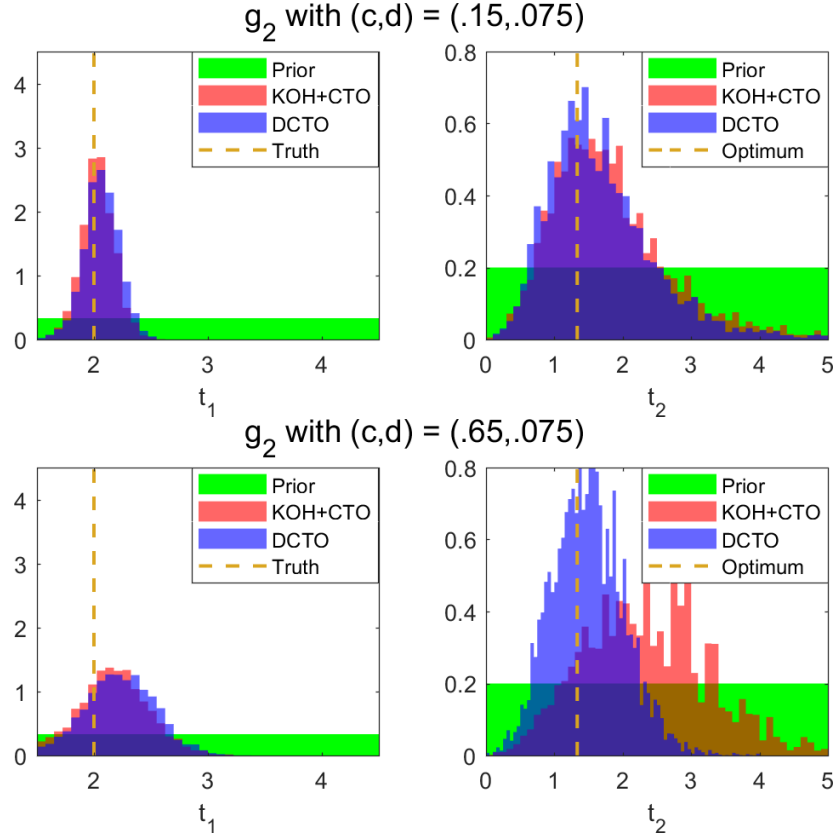


Figure 6: Prior and posterior distributions of the calibration parameter θ_1 and design parameter θ_2 , along with their true/optimal values, for DCTO and KOH+CTO in the case of true systems g_2 . The top row corresponds to a smaller discrepancy, with $(c,d) = (.15,.075)$; the bottom row corresponds to a larger discrepancy, with $(c,d) = (.65,.075)$.

two settings of c . By contrast, and less surprisingly, the posterior distributions for θ_1 are somewhat wider in the case of g_2 , for each of the two settings of (c, d) . Nonetheless, the posterior distributions for g_2 , as for g_0 and g_1 , still peak at the true value of θ_1 and at the optimal value of θ_2 under DCTO. The case of g_2 with $(c, d) = (.65, .075)$ is the only case in which DCTO and KOH+CTO produce strikingly different results. Here, DCTO supplies a posterior distribution for θ_2 that peaks at the true optimum, while KOH+CTO produces a much wider distribution that fails to peak at the optimum. The reason for this difference is unclear. DCTO and KOH both have fairly high uncertainty in the posterior distribution of θ_1 , which propagates to uncertainty in the posterior distribution of θ_2 , since the optimal θ_2 is dependent upon the true value of θ_1 . It is possible that this affects KOH+CTO more than DCTO since DCTO is able to use the information contained in the true observations of g_2 to inform the design of θ_2 , whereas under KOH+CTO the true observations are used only in calibration of θ_1 and not in the design of θ_2 .

Matters change in the case of g_3 , where the calibration procedure is somewhat unsuccessful for both DCTO and KOH+CTO. Figure 7 (upper left) shows that the true value of θ_1 is well into the tails of the posterior distributions. Surprisingly, increasing d from 0 to 0.1 and keeping $c = 0.055$, the results are significantly better, even though the discrepancy in this case is larger. In the lower left of Figure 7, we see that the posterior distributions again peak sharply near the true value of θ_1 . In all versions of the discrepancy function explored here, the posterior distribution under DCTO is roughly similar with respect to θ_2 ; wider than the posteriors for θ_1 , but peaking near the optimal θ_2 even when this is not true of θ_1 .

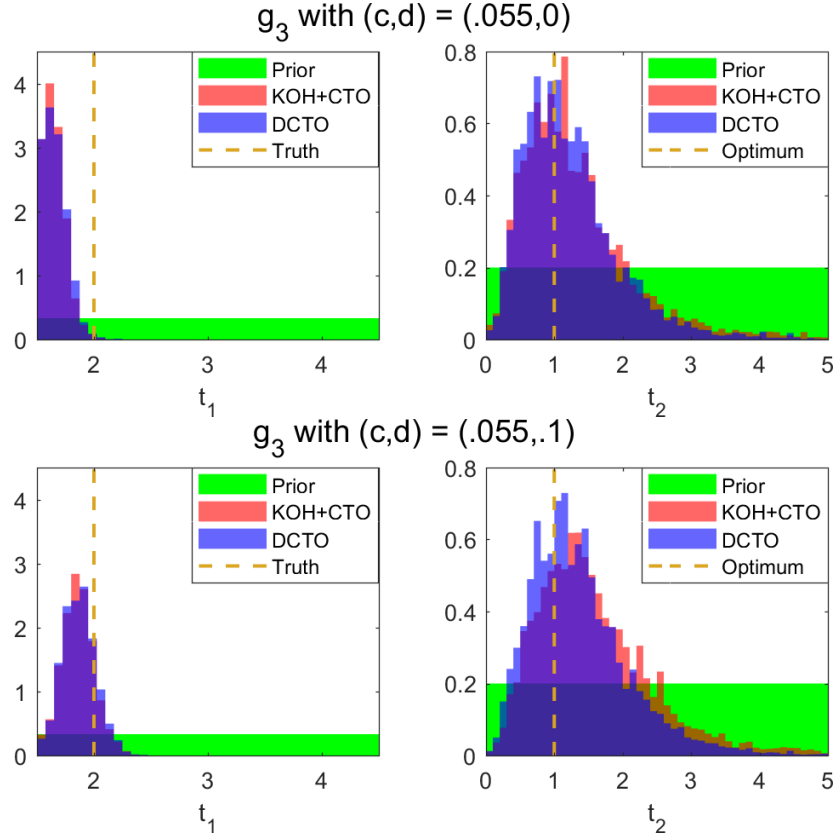


Figure 7: Prior and posterior distributions of the calibration parameter θ_1 and design parameter θ_2 , along with their true/optimal values, for DCTO and KOH+CTO in the case of true systems g_3 . The top row corresponds to a smaller discrepancy, with $(c, d) = (.055, 0)$; the bottom row corresponds to a larger discrepancy, with $(c, d) = (.055, .1)$.

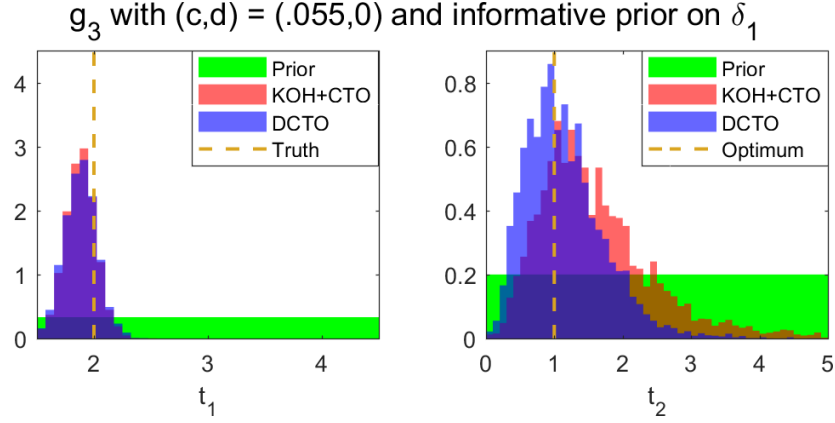


Figure 8: Prior and posterior distributions of the calibration parameter θ_1 and design parameter θ_2 , along with their true/optimal values, for DCTO and KOH in the case of true systems g_3 with $(c, d) = (.055, 0)$ and an informative prior for δ_1 .

In order to achieve better results in the case of g_3 with $d = 0$, we attempted to place a more informative prior on the discrepancy function δ_1 . We pursued two different strategies to do this. Firstly, we integrated the discrepancy $g_3 - f$ over the supports of x and t_2 , finding the average value of the discrepancy. We then re-ran DCTO using $m_1(x, t_2) = (\int (g_3(z, \theta_1, w) - f(z, \theta_1, w)) dz dw) / 2.5$ as the (constant) mean of the GP prior on δ_1 . This corresponds to a case in which one knows on average how far one's model tends to be from the true system. The results, however, were not appreciably different from the original results using a mean of 0 for the GP prior on δ_1 . Secondly, we again ran DCTO using $m_1(x, t_2) = g_3(x, \theta_1, t_2) - f(x, \theta_1, t_2)$, so that the GP prior mean on δ_1 was the true discrepancy. This corresponds to a case in which one has (e.g. through extensive experimentation) a more thorough understanding of the form of the model's discrepancy with the true system. This second strategy proved fruitful, producing the results in Figure 8. KOH+CTO and DCTO were equally successful in calibration, but DCTO again outperforms KOH+CTO on design here, with a posterior which is both narrower and more

centered on the true optimum. Given that the two design procedures perform similarly with an uninformative prior on δ_1 , it's unclear why using an informative prior produces such different design results, especially since the informative prior has an almost identical effect in improving the calibration results in the two cases.

The posterior predictive distributions under DCTO and KOH+CTO are very close under six of the eight discrepancies studied. Nonetheless, in most of those six cases DCTO enjoys very slightly narrower posterior predictive distributions. In the two cases under which DCTO and KOH+CTO diverge appreciably, DCTO enjoys much better results, with sharper distributions that center nearer to the true optimal model output. Figure 9 shows the posterior predictive distributions for g_0 , the case of no model discrepancy, and for two settings of g_1 , the case of multiplicative model discrepancy. Here, the posterior predictive distributions for DCTO and KOH+CTO overlap almost perfectly, except for the slightly higher peaks of DCTO.

Figure 10 shows the results for two settings of g_2 , an additive discrepancy form. For the smaller discrepancy setting of g_2 , the results are similar to those for g_0 and g_1 , with DCTO enjoying slightly less uncertainty. The larger discrepancy setting for g_2 is the same case as that shown in Figure 6, where KOH+CTO performs well with respect to calibration but poorly with respect to design. Figure 10 shows that this poor design corresponds to wildly different predictive performance between DCTO and KOH+CTO, with KOH+CTO suffering from high uncertainty and strange multimodal behavior for some levels of the control input x . It is however notable that even here, the posterior predictive distribution's global mode still occurs at the same location as the global mode under DCTO, despite the

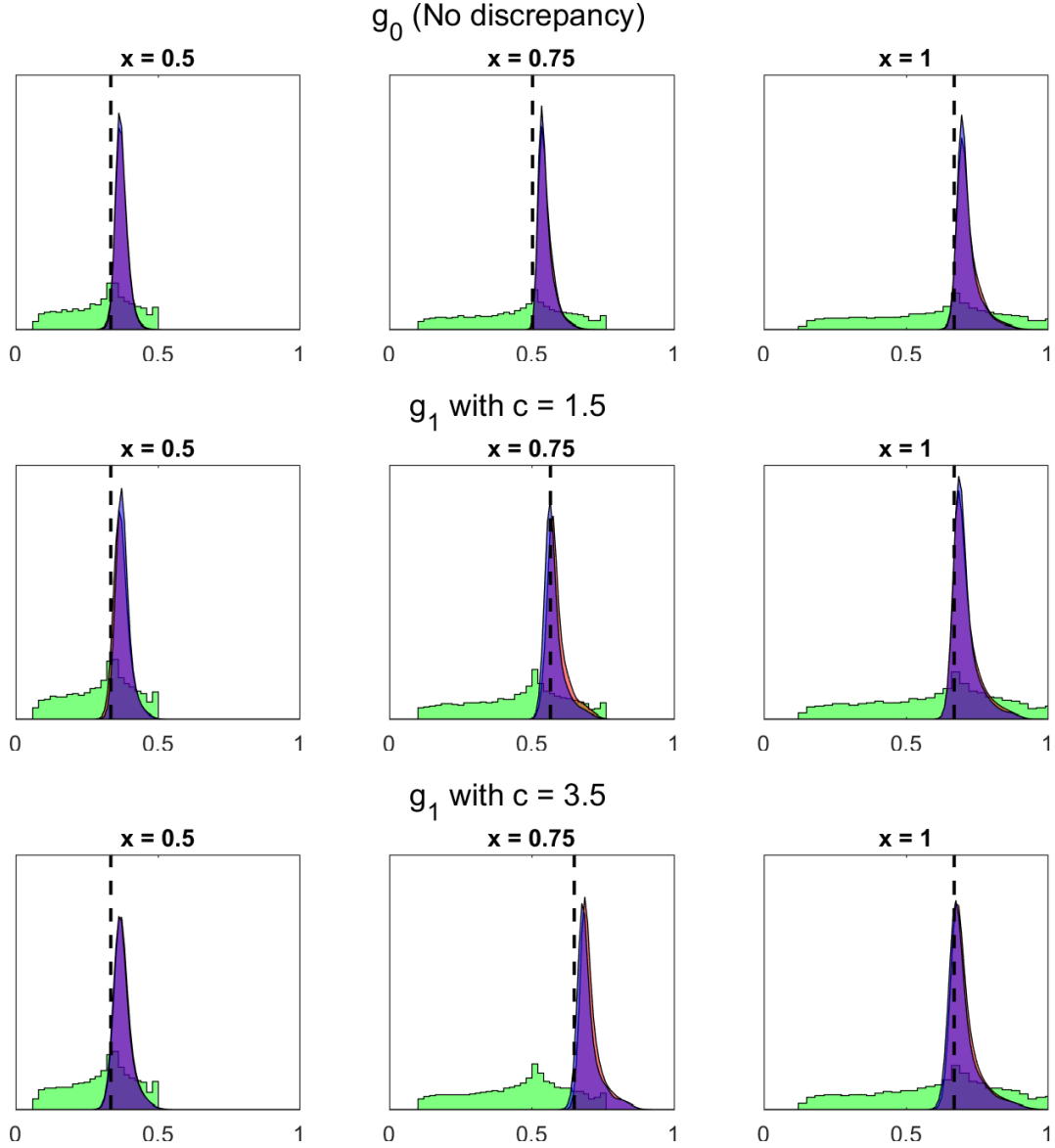


Figure 9: Prior (green) and posterior predictive distributions of the model output, along with the optimum, for DCTO and KOH+CTO at three values of the control input x . The red KOH+CTO and blue DCTO distributions overlap almost perfectly, but in all cases except the bottom middle plot, DCTO peaks just slightly above KOH+CTO.

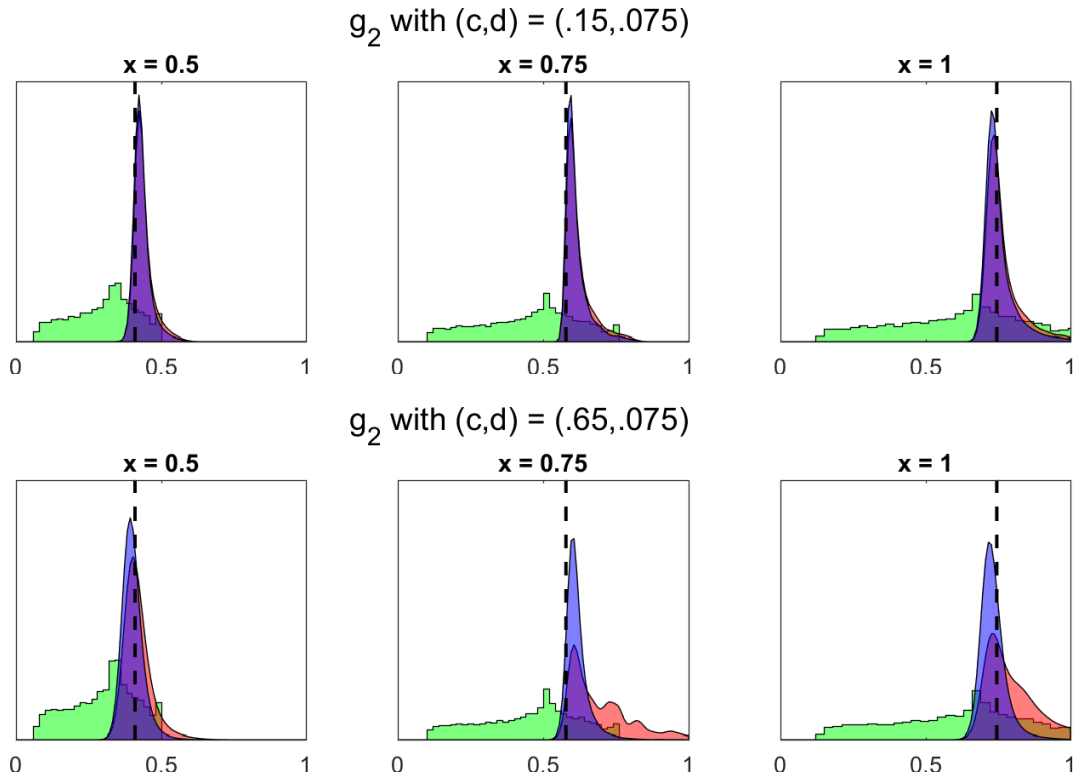


Figure 10: Prior (green) and posterior predictive distributions of the model output, along with the optimum, for DCTO and KOH+CTO at three values of the control input x .

fact that this is not true of the posterior distributions of the design parameter t_2 under the two techniques.

The additive discrepancy form of g_3 again has similar posterior predictive results under DCTO and KOH+CTO for both small and large versions of the discrepancy, except when an informative prior is supplied for the discrepancy function. Recall that the small discrepancy version of g_3 is a case in which both DCTO and KOH performed poorly with respect to calibration, as shown in Figure 7. The top row of Figure 11 shows that this poor calibration does not result in similarly poor predictive performance. The improved calibration that results from applying an informative prior, as shown in Figure 8, inflates the posterior uncertainty surrounding the design variable t_2 for KOH+CTO, while slightly deflating the t_2 uncertainty for DCTO. Figure 11 (middle row) seems to show that this difference between KOH+CTO translates to similar differences in posterior predictive distributions when using the informative prior: slightly less uncertainty under DCTO, slightly more under KOH+CTO. However, despite the fact that both techniques experience dramatically better calibration under the informative prior than without it, there is not a similarly dramatic difference between the posterior predictive distributions with and without the informative prior, under either technique. The flexibility of the discrepancy term in CTO allows for accurate prediction even when the calibration is inaccurate.

The calibration, design, and predictive results for all seven cases (one case of zero discrepancy plus two versions each of three different forms of discrepancy) are summarized in Table 1. The top table shows the posterior variances of the calibration parameter t_1 , the design parameter t_2 , and the predictive distribution \tilde{y} at control setting $x = 0.75$.

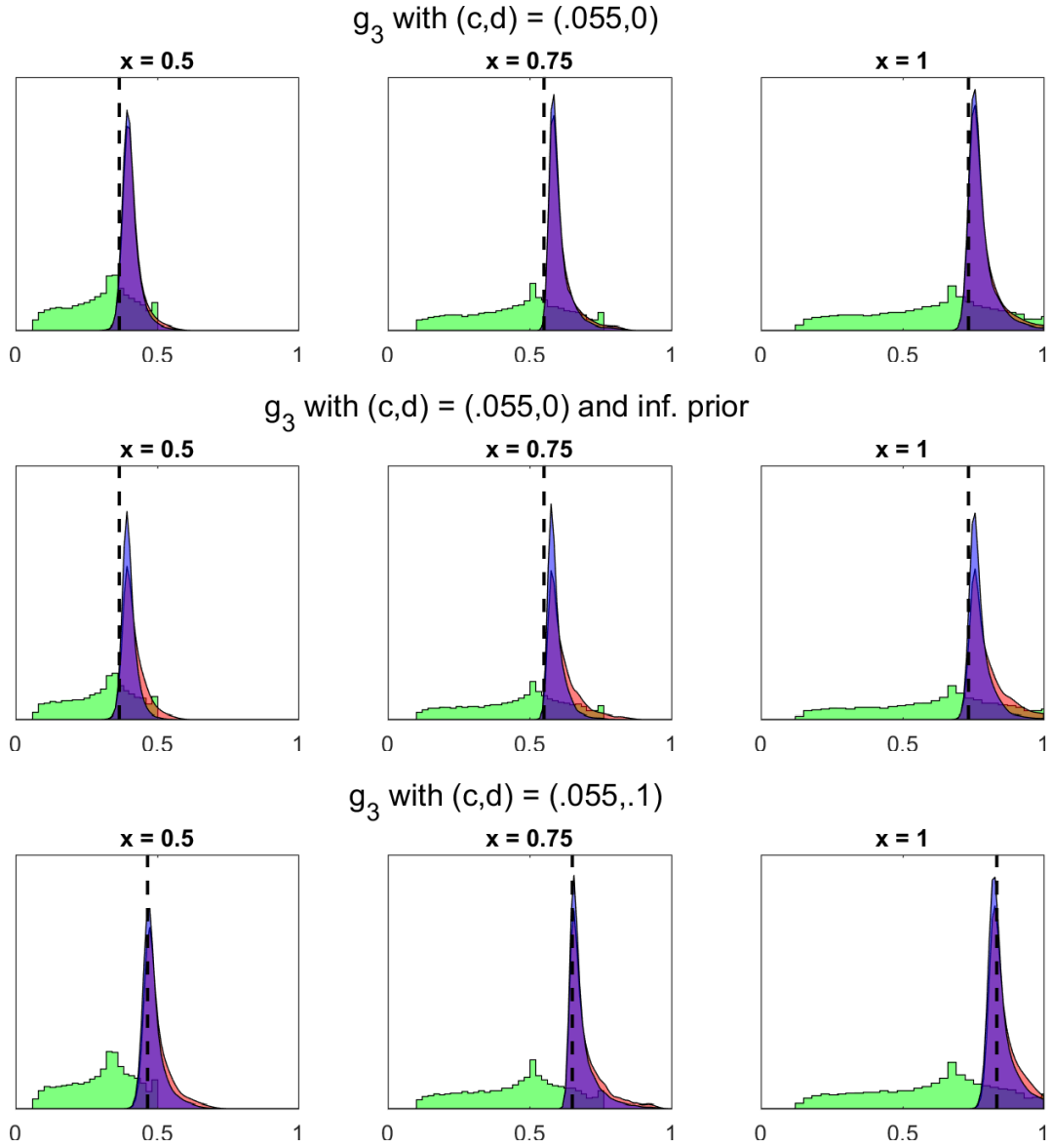


Figure 11: Prior (green) and posterior predictive distributions of the model output, along with the optimum, for DCTO and KOH+CTO at three values of the control input x .

Discrepancy	t_1 variance		t_2 variance	
	DCTO	KOH+CTO	DCTO	KOH+CTO
0	0.0198	0.0179	0.6636	0.7066
1, small	0.0181	0.0131	0.5881	0.7055
1, large	0.0129	0.0096	0.7676	0.7465
2, small	0.0233	0.0209	0.5849	0.7022
2, large	0.0896	0.0872	0.2711	0.7992
3, small	0.0108	0.0093	0.4903	0.6257
3, large	0.0216	0.0207	0.5228	0.7009
3, small, inf.	0.0201	0.0179	0.3330	0.6787

Discrepancy	$ \theta_1 - \hat{\theta}_1 $		$ \theta_2 - \hat{\theta}_2 $	
	DCTO	KOH+CTO	DCTO	KOH+CTO
0	0.0969	0.1124	0.2594	0.2838
1, small	0.0007	0.0427	0.2720	0.3816
1, large	0.0436	0.0001	0.3614	0.4361
2, small	0.0686	0.0353	0.3365	0.4664
2, large	0.2346	0.1808	0.1577	1.0270
3, small	0.3393	0.3464	0.2304	0.3090
3, large	0.1325	0.1403	0.3651	0.5781
3, small, inf.	0.1151	0.1157	0.1488	0.5921

Table 1: Posterior variances and mean absolute deviations for the calibration variable θ_1 and the design variable θ_2 . The estimator $\hat{\theta}_i$ is the posterior mean of t_i . The final line in each table gives the results for the use of an informative prior for the discrepancy of g_3 with $(c, d) = (0, .055)$.

The bottom table shows the absolute deviation of the resulting posterior means $\hat{\theta}_1, \hat{\theta}_2$, and \hat{y} from their known true values. It appears that KOH produces narrower calibration posteriors than DCTO, as the variances for θ_1 are uniformly lower for KOH, if usually only slightly. However, when we instead look at $|\theta_1 - \hat{\theta}_1|$, matters are less clear. DCTO has a lower calibration estimate absolute error in five of the eight cases studied here, and in general, the differences between the two procedures here is small. It thus appears that DCTO and KOH+CTO enjoy similar levels of success in calibration. Clearer differences emerge in looking at the performance of the two procedures with respect to the design

variable. DCTO produces a smaller posterior variance in seven out of the eight cases, in two cases more than halving the variance produced under KOH+CTO. The difference is even more pronounced for $|\theta_2 - \hat{\theta}_2|$ under the two procedures, as DCTO produces a lower absolute error in each of the eight cases, sometimes strikingly so. For example, in the large discrepancy version of g_2 , DCTO produces an estimate with less than one sixth the absolute error of KOH+CTO. It appears that DCTO and KOH+CTO perform similarly with respect to calibration, but that DCTO produces superior results with respect to design.

References

Kennedy, M. C. and A. O'Hagan (2001). Bayesian calibration of computer models. *Journal of the Royal Statistical Society: Series B* 63(3), 425–464.